On the Equivalence of LEO-SAR Constellations and Complex High-Orbit SAR Systems for the Monitoring of Large-Scale Processes

Jalal Matar, Marc Rodriguez-Cassola, Gerhard Krieger, *Fellow, IEEE*, and Alberto Moreira, *Fellow, IEEE*

***Abstract*— High Earth orbit synthetic aperture radar (SAR) systems offer high temporal sampling and moderate spatial resolution on a global scale, potentially outperforming conventional low Earth orbit (LEO) systems in revisit times. However, this requires complex system architectures such as burst operation modes with multiple subswaths, large antennas, and digital beamforming. Similar temporal sampling and coverage enhancements can be realized with constellations of classical monostatic SAR instruments in LEO. This letter compares the complexity of such equivalent monostatic LEO-SAR constellations to complex high-altitude SAR systems and provides design numbers for two medium Earth orbit (MEO)-SAR mission examples and their LEO counterparts.**

***Index Terms*— Constellations, medium Earth orbits (MEOs), small satellites, synthetic aperture radar (SAR), system performance.**

I. Introduction

SYNTHETIC aperture radar (SAR) missions in high Earth orbit offer compelling solutions for applications requiring frequent monitoring and medium resolution, such as climate modeling, hazard surveillance, and reconnaissance. Broadly, these missions can be classified into two categories: lower altitude medium Earth orbit (MEO) systems, under 10 000 km, recognized for their extensive coverage and near-global reach, and higher altitude MEO systems extending to geosynchronous orbits, noted for their persistent imaging ability on local scales. A range of MEO-SAR missions can be developed targeting global-scale measurement of soil moisture and surface deformation using a single satellite, such as the 5952-km mission concept introduced in [1], or continental-scale measurements with bidaily revisits from 20 000 km, or lower latitudes (below ±40°) from near-equatorial inclinations.

The systems required for the above MEO missions are intricate and massive, driven by the increased free-space propagation loss and launch costs. These challenges are mitigated using larger antenna structures, digital beamforming, and electric propulsion for progressive orbit raising from low Earth orbit (LEO). This situation introduces an opportunity for competitive low-altitude constellations composed of simpler, lighter satellites. Each satellite within the constellation uses lightweight antenna structures, simple operation modes such as stripmap, and avoids digital beamforming and onboard processing. Like NewSpace SAR systems [2], these constellations use identical instruments installed on small commercial platforms to leverage economies of scale. A collective launch of small satellites is anticipated for such configurations.

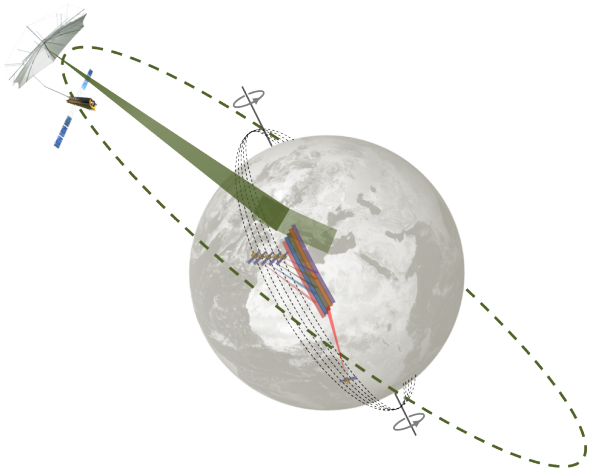

Fig. 1. Realization of a LEO constellation of simple SAR satellites equivalent to a high-altitude MEO-SAR system.

This letter explores the equivalence between MEO-SAR systems and LEO-SAR constellations. It offers a comparison illustrated by two realistic mission concepts. Fig. 1 demonstrates a realization of a LEO constellation that parallels the performance of a high-altitude, wide-swath MEO-SAR system. The individual elements of the constellation can cover narrower swaths that accumulate to that of the higher altitude systems. The acquisitions can be simultaneous, nonsimultaneous, or squinted to achieve equivalent performance.

The remainder of this letter is structured as follows. Section II presents the theoretical framework for deriving LEO-SAR constellations. Section III provides examples of two low-altitude and high-altitude polarimetric and interferometric MEO-SAR missions using very refined SAR instruments and includes a derivation and comparison of the equivalent LEO constellations. This letter is closed with an outlook in Section IV.

Manuscript received 18 July 2023; revised 17 November 2023; accepted 24 November 2023. Date of publication 27 November 2023; date of current version 19 December 2023. *(Corresponding author: Jalal Matar.)*

The authors are with the Microwaves and Radar Institute, German Aerospace Center (DLR), 82234 Weßling, Germany (e-mail: jalal.matar@dlr.de).

Digital Object Identifier 10.1109/LGRS.2023.3337042

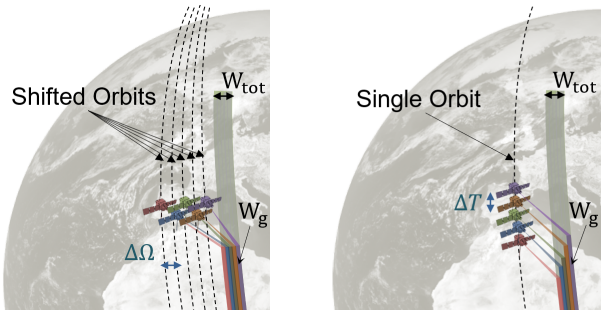

(a) (b)

Fig. 2. Example orbit formations of monostatic SAR constellations for swath distribution. The individual platforms are flying on (a) orbits whose right ascension of ascending node is shifted by $\Delta\Omega$ and (b) single orbital plane with a time delay ΔT.

II. Equivalent Monostatic SAR Constellations

As it is widely known, the size of an SAR antenna results from the simultaneous optimization of power demand, swath width, incident angle range, azimuth and range resolutions, and ambiguity rejection capabilities [3], [4]. Deviations from the nominal values relevant to the applications—for instance, broader swaths, increased range of incident angles, or improved resolutions—typically increase system complexity, which results in larger antenna sizes and the use of analog and digital beamsteering capabilities [5], [6]. The increase in system complexity can be mitigated using monostatic constellations, in which each element covers a portion of the total swath (W_{tot}) and the orbit duty cycle. Using N satellites, we can express

$$N = \left\lceil \frac{W_{\text{tot}}}{W_{\text{g}} \cdot (1 - \alpha(\theta_{\text{lat}}))} \right\rceil \tag{1}$$

as a function of the swath covered by the single satellite (W_{g}) and a design factor α which controls the overlap between consecutive subswaths at a specific latitude (θ_{lat}). Furthermore, the antenna's surface can be designed to cover the individual swaths in the stripmap mode, eliminating the need for beamsteering or beamforming capabilities.

A. Orbit Formation

In terms of orbit design, several strategies can achieve cumulative swath coverage given specific revisit interval requirements.

For simultaneous imaging of wide swaths, constellation elements can be arranged in adjacent orbital planes with zero along-track baselines, as illustrated in the left plot of Fig. 2. This is achieved by shifting the right ascension of the ascending node (RAAN) of neighboring orbits by

$$\Delta\Omega \approx \frac{W_{\text{g}} \cdot (1 - \alpha(\theta_{\text{lat}}))}{R_{\text{E}} \cdot \cos\theta_{\text{lat}} \cdot |\sin\theta_{\text{N}}(\theta_{\text{lat}})|} \tag{2}$$

where θ_{N} stands for the northing angle (angle between the line-of-sight projection on the local tangent plane and the local north vector), and R_{E} denotes Earth's equatorial radius. $\Delta\Omega$ is estimated at the equator for gap-free global coverage, resulting in more swath overlap at higher latitudes. This aspect facilitates individual system management and reduces the overall orbit duty cycle if redundant samples are not desired.

Alternatively, for semi-simultaneous imaging, constellation elements can adopt different along-track baselines, corresponding to temporal lags in the order of several tens of seconds, within the same orbital plane as illustrated in the right plot of Fig. 2. The time lag

$$\Delta T(\theta_{\text{lat}}) = \frac{\Delta\Omega(\theta_{\text{lat}})}{\omega_{\text{E}}} \tag{3}$$

between consecutive platforms is optimized for θ_{lat} while leveraging Earth's angular velocity (ω_{E}). The time lag varies along the orbit as a function of latitude, creating regions with different overlap degrees. This can reduce the overall orbit duty cycle, similar to the previous approach. While other formations are possible, they result in non-simultaneous imaging of the total swath.

The entire constellation can be launched with a minimal number of launchers, typically one, directly to the desired or lower parking orbit. Individual spacecraft are raised to their final orbit at separate intervals in the latter to achieve the required drifts. Some existing constellations—including ICEYE, Capella, and Starlink—use such procedures.

A single-element failure results in around $100/N\%$ loss in total coverage, yet it does not compromise mission continuity. Mitigation measures include adjusting the acquisition plan, performing roll maneuvers, or modifying the formation flight configuration, albeit with a slight reduction in temporal coverage and a potential increase in fuel consumption.

B. Equivalent Systems

In this letter, two SAR systems are considered equivalent if they have the same system imaging capacity, data quality, and revisit frequency over predefined regions of interest. System imaging capacity refers to the average samples collected per second, while data quality is assessed by resolution, ambiguity ratios, and sensitivity.

The imaging capacity of an individual satellite is driven by available energy, which restricts the orbit duty cycles of complex systems. By addressing inefficiencies related to antenna (e.g., surface utilization during transmission and reception), imaging mode (e.g., stripmap versus ScanSAR), instrument design (e.g., reducing lossy elements), propagation, and redundant coverage, a reduction of over 10 dB in the power budget can be achieved. This reduction can be leveraged to decrease the spacecraft's antenna size and overall power consumption. Such optimization is feasible for individual constellation elements since the hardware design can be tailored to cover narrow subswaths.

In general, a constellation composed of N narrow-swath high-efficiency satellites can be designed to achieve equivalence with a wide-swath SAR system at different altitudes.

III. Mission Examples

This section presents LEO constellations equivalent to two reference MEO-SAR concepts. The first targets global coverage from a 5952-km high orbit, as previously introduced

TABLE I
RELEVANT PARAMETERS OF A REFERENCE MEO-SAR SYSTEM AT 5952 km TARGETING GLOBAL COVERAGE

Parameter	Value
Cycle length [days]	3
Orbital inclination [deg]	122
Altitude at equator [km]	5952
Average power [W]	350
Transmit duty cycle [%]	8
Swath width [km]	1667
Incident angle range [deg]	[20, 47]
Acquisition mode	ScanSAR
Antenna type	reflector
Antenna diameter [m]	22
Feeding elements	120
System bandwidth [MHz]	< 22
Frequency [GHz]	5.405
Two-way losses [dB]	4
Noise Figure [dB]	3
Backscatter law	Ulaby (Short Vegetation)
2-D SLC resolution [m^2]	57×20
NESN [dB]	< -22
ASR [dB]	< -22

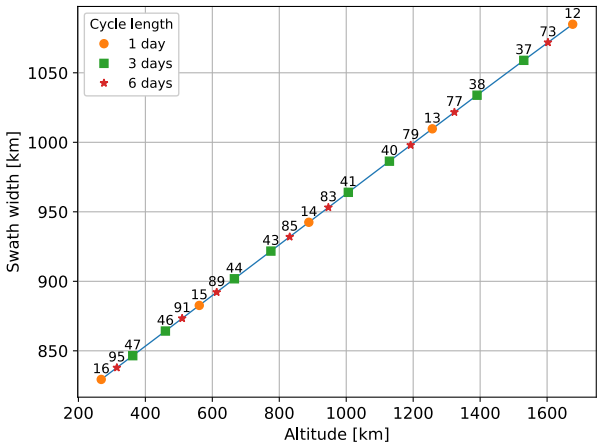

Fig. 3. Swath width required for gap-free equatorial coverage within three days from one-, three- and six-day repeat low-Earth SSOs. The numbers on the graph represent orbital revolutions in a repeat cycle.

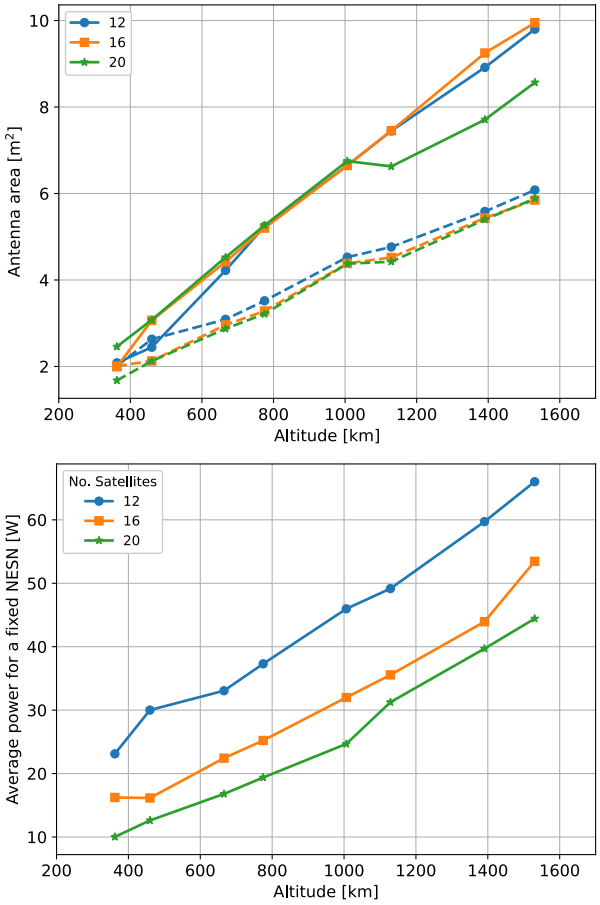

Fig. 4. (Top) Variation in antenna area and (bottom) average transmit power with altitude for 12-, 16-, and 20-satellite constellations in SSO. The top plot compares planar (solid lines) and parabolic surfaces (dashed lines). The data represents C-band systems designed for global coverage, achieving performance equivalent to the reference MEO system.

in [1]. The second targets local/continental coverage from higher altitudes (e.g., 20 200 km) and is introduced in this letter. We provide precise design numbers for constellation sizes and system parameters as a result of the analysis.

A. Global MEO-SAR and Its Equivalent Monostatic LEO-SAR Constellation

The reference mission described in [1], with the parameters detailed in Table I, targets global coverage from a three-day repeat ground track orbit for applications such as soil moisture and large-scale 3-D deformation monitoring (e.g., with a target accuracy of a few mm/year after four years of averaging [7]). The suggested C-band SAR instrument is reasonably complex. It requires a 22-m reflector antenna with an extensive feeding network, elevation beamforming, and a ScanSAR imaging mode to cover the 1667-km wide swath.

LEO altitudes reduce free-space propagation losses and the need for wide instantaneous swaths due to increased beam velocity. Fig. 3 shows the required swath for global coverage from low-Earth sun-synchronous orbits (SSOs) with different repeat cycles. Alternative cycles (e.g., one- or six-day repeat) allow for extended altitude sampling and enable optimizing the mission according to the launch and acquisition strategy. For global coverage, shorter cycles will require daily roll maneuvers. Sun-synchronicity is chosen for improved energy efficiency and accessibility to polar latitudes. However, high inclinations degrade deformation measurements accuracy in the north–south direction for single-satellite acquisitions (e.g., an order of magnitude worse than the up–down and east–west directions) [8]. Two options are suggested to partially regain accuracy: 1) use D satellites of the constellation for squinted acquisitions and 2) use D satellites of the constellation for bistatic acquisitions over areas of interest at the cost of $<100 \cdot D/N\%$ coverage loss.

Fig. 4 depicts the variation in antenna area (top) and average transmit power (bottom) for a single constellation element operating in the stripmap mode with 12, 16, or 20 satellites. The variations are observed for the three-day repeat orbits and swath combinations described in Fig. 3, with a 25° incidence at near range. The performance of the constellation elements aligns with the reference MEO system specified in Table I, i.e., a worst case ambiguity-to-signal ratio (ASR) of -22 dB,

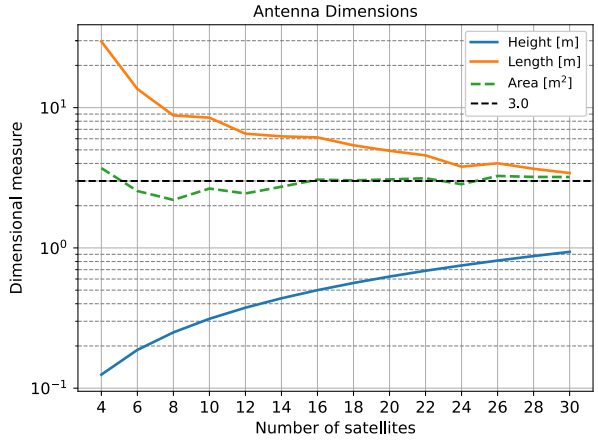

Fig. 5. Antenna dimensions required to achieve a worst case ASR of −22 dB for LEO constellations at 460 km, equivalent to the reference MEO-SAR satellite at 5952 km. The analysis assumes a near incidence of 25°.

worst case noise equivalent sigma nought (NESN) of −22 dB and a 2-D resolution of 1140 m^2. The required swath width per element (W_g) ranges from 40 to 90 km, derived according to (1), and can be achieved without gaps for the provided designs.

The antenna areas in Fig. 4 (top) are plotted for two design cases: 1) planar antennas with low complexity and sinc patterns in solid lines and 2) parabolic antenna surfaces (or equivalent weighting) with better sidelobe suppression in dashed lines. The use of the latter case allows for reducing the antenna area by around 30%; however, it comes at the cost of an increase in system complexity and average power. The antenna area increases linearly with altitude for both the designs, driven by the required ambiguity suppression. Deviations from this linear behavior, as seen in the case of 20 satellites shown in the green curve in Fig. 4 (top), are caused by the differences in the power of range ambiguities. The trends can be extended to other constellation sizes; however, the three presented examples represent feasible systems in terms of the required gap-free swath, antenna dimensions, and power.

Based on these trends, we chose the orbit at 460-km altitude for the equivalent constellation. While this altitude does lead to instrument and power requirements above the minimum values shown in Fig. 4, it offers advantages in terms of spacecraft wet mass. At lower altitudes, the increased atmospheric drag and orbit decay rate might require more frequent on-ground operations/maneuvers, ultimately outweighing the benefits of smaller instruments in mass reduction. Fig. 5 illustrates the variation in antenna dimensions needed to cover the corresponding 866-km swath as the constellation grows. The antenna height is determined based on the 3-dB beamwidth needed to cover the swath portion. Using this height, the PRF is optimized to achieve range ambiguity ratios better than −25 dB. Subsequently, the antenna length is derived from the resulting PRF, taking into account the azimuth ambiguity ratio requirement.

Table II lists the main system parameters and performance metrics for the 12-, 16- and 20-element constellations

TABLE II
SYSTEM AND PERFORMANCE METRICS FOR 12-, 16- AND 20-ELEMENT CONSTELLATIONS AT 460 km IN STRIPMAP MODE

Parameter	12 Sat.	16 Sat.	20 Sat.
Individual swath [km]	73.51	55.12	44.1
Incident angle range [deg]	25 - 32.74	25 - 30.9	24.3 - 29.11
Antenna length [m]	7.33	6.22	5.63
Antenna height [m]	0.37	0.5	0.62
PRF [Hz]	1888	2150	2435
Doppler bandwidth [Hz]	593	698	772
Azimuth resolution [m]	15.62	13.26	12
Range resolution [m]	73	86	95
Average power [W]	25	16	11
Two-way losses [dB]	1.5	1.5	1.5

operating in the stripmap mode. Timing parameters have been adjusted to avoid nadir returns at equatorial latitudes. Potential limitations by nadir echoes at different latitudes could be suppressed, without additional cost, by applying the dual-focusing nadir suppression technique using up- and down-chirps [9]. All the constellations meet the ASR and NESN requirements of the reference while assuming a similar noise figure. A 2.5-dB reduction in the system losses is assumed compared with the reference to account for the simplification in the antenna front-end and electronics. The range resolution is adjusted to maintain the pixel area consistent with the reference. The reduced swath width is advantageous in terms of power consumption and allows for shorter antenna lengths due to improved ambiguity ratios at higher PRFs, but it comes at the expense of a larger constellation and an asymmetrical pixel size. The required satellites for these systems seem to be in the class of 50–100 kg with large orbit duty cycles.

B. High MEO-SAR and Its Equivalent Monostatic LEO-SAR Constellation

Operating in the L-band at an altitude of around 20 200 km, this reference mission aims to monitor soil moisture and surface deformation across Europe on a subdaily basis, using full polarimetric and interferometric observations. The unique altitude allows two daily revisits over large overlap regions between ascending and descending passes. Table III details the orbit and system parameters.

The SAR instrument uses a 25-m reflector antenna fed by a network of 17 × 6 L-band patches in elevation and azimuth, respectively. Every set of six azimuth patches is connected to a single transmit/receive module, which allows refocusing of the received beam at the edges of the 2115-km swath. The system achieves a total ASR better than −28 dB along both the range and azimuth and an NESN better than −25 dB.

The orbit selection for the equivalent LEO constellation follows the trends in Fig. 3. The one-day repeat SSO at 561 km presents a good tradeoff between the required instrument size and the on-ground operations and maneuvers. The accuracy of the north–south deformation measurements can be improved similar to the previous example. To achieve twice-daily, gap-free coverage of Europe, a total swath of 2172 km is required and will be distributed among the constellation elements. Fig. 6 presents the resulting antenna dimensions for various constellation sizes, designed as per Section III-A to maintain

TABLE III

RELEVANT PARAMETERS OF A REFERENCE MEO-SAR SYSTEM AT 20 200 km COVERING EUROPE

Parameter	Value
Cycle length [days]	1
Orbital inclination [deg]	69.1
Altitude at equator [km]	20182
Average orbit duty cycle (Europe) [%]	22
Average power [W]	165
Transmit duty cycle [%]	8
Swath width [km]	2115
Incident angle range [deg]	[18, 42]
Acquisition mode	ScanSAR
Antenna type	reflector
Antenna diameter [m]	25
Frequency [GHz]	1.2575
Two-way losses [dB]	3
Noise Figure [dB]	3
Backscatter law	Ulaby (Soil & Rock)
2-D SLC resolution [m^2]	20×500
NESN [dB]	< -25
ASR [dB]	< -25

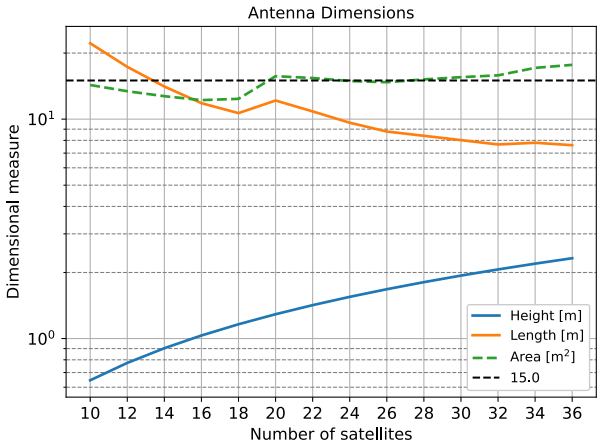

Fig. 6. Required antenna dimensions to achieve a worst case ASR of −25 dB for LEO constellations at 561 km, equivalent to the reference MEO-SAR satellite at 20 200 km. The analysis assumes a near incidence of 25°.

TABLE IV

SYSTEM AND PERFORMANCE METRICS FOR 18-, 24- AND 30-ELEMENT CONSTELLATIONS AT 561 km IN STRIPMAP MODE

Parameter	18 Sat.	24 Sat.	30 Sat.
Individual swath [km]	123.1	92.26	73.8
Incident angle range [deg]	25 - 35.56	25 - 33.10	25 - 31.56
Antenna length [m]	10.65	9.63	8.02
Antenna height [m]	1.17	1.55	1.94
PRF [Hz]	1300	1500	1742
Doppler bandwidth [Hz]	404.82	447.2	537.43
Azimuth resolution [m]	22.37	20.25	16.55
Range resolution [m]	447	494	593.5
Average power [W]	3.2	1.85	1.4
Two-way losses [dB]	1.5	1.5	1.5

total ambiguity ratios better than −25 dB. The non-linear behavior of the antenna length, evident for 20 satellites, results from the differences in the power of range ambiguities.

Table IV lists the main system parameters and performance metrics for the 18-, 24- and 30-element constellations operating in the stripmap mode, using the antenna dimensions provided in Fig. 6. All the cases meet the ASR and NESN requirements of the reference, assuming a 3-dB noise figure and 1.5-dB system losses. Larger constellation sizes are advantageous when the platform or available fairing restricts larger antenna dimensions. The range resolution is adjusted to maintain the reference pixel area. Nevertheless, the low power demand and orbit duty cycle to cover Europe (around 22%) give room to improve the range resolution and system capacity compared with to the reference. For example, increasing the average power to around 67, 47, and 48 W would result in squared pixel areas of $(22\ \text{m})^2$, $(20\ \text{m})^2$, and $(17\ \text{m})^2$ for the three examples, respectively.

IV. OUTLOOK

This letter discusses the equivalence of constellations of small LEO-based SARs and refined SAR systems operating in high orbits. The presented MEO-SAR systems are attractive for their large accessibility and potential to provide global and continental coverage with short repeat duration and moderate resolution using a single satellite. However, this comes at the expense of reduced power and system efficiencies, e.g., increased free-space propagation loss, complex instruments, and launch to high orbits.

The letter shows that wide-swath high-orbit systems can be exchanged by a constellation of highly efficient LEO-SAR systems, achieved by distributing the large access areas among individual elements. The equivalence is demonstrated through realistic MEO-SAR system examples and design numbers for the constellations regarding antenna sizes, swath widths, and achievable SAR performance.

ACKNOWLEDGMENT

The authors would like to thank Valeria Gracheva and Martin Suess from ESA for the fruitful discussions on the derivation of LEO constellations.

REFERENCES

[1] J. Matar, M. Rodriguez-Cassola, G. Krieger, P. López-Dekker, and A. Moreira, "MEO SAR: System concepts and analysis," *IEEE Trans. Geosci. Remote Sens.*, vol. 58, no. 2, pp. 1313–1324, Feb. 2020.

[2] M. Villano et al., "NewSpace SAR: Disruptive concepts for cost-effective SAR system design," in *Proc. 13th Eur. Conf. Synth. Aperture Radar*, Mar. 2021, pp. 1–6.

[3] J. Curlander and R. McDonough, *Synthetic Aperture Radar*, vol. 11. New York, NY, USA: Wiley, 1991.

[4] A. Freeman et al., "The 'myth' of the minimum SAR antenna area constraint," *IEEE Trans. Geosci. Remote Sens.*, vol. 38, no. 1, pp. 320–324, Mar. 2000.

[5] A. Freeman et al., "SweepSAR: Beam-forming on receive using a reflector-phased array feed combination for spaceborne SAR," in *Proc. IEEE Radar Conf.*, 2009, pp. 1–9.

[6] N. Gebert, G. Krieger, and A. Moreira, "Multichannel azimuth processing in ScanSAR and Tops mode operation," *IEEE Trans. Geosci. Remote Sens.*, vol. 48, no. 7, pp. 2994–3008, Jul. 2010.

[7] J. Matar, M. Rodriguez-Cassola, G. Krieger, M. Zonno, and A. Moreira, "Potential of MEO SAR for global deformation mapping," in *Proc. 13th Eur. Conf. Synth. Aperture Radar*, Mar. 2021, pp. 1–5.

[8] P. Prats-Iraola, P. Lopez-Dekker, F. De Zan, N. Yagüe-Martínez, M. Zonno, and M. Rodriguez-Cassola, "Performance of 3-D surface deformation estimation for simultaneous squinted SAR acquisitions," *IEEE Trans. Geosci. Remote Sens.*, vol. 56, no. 4, pp. 2147–2158, Apr. 2018.

[9] M. Villano, G. Krieger, and A. Moreira, "Nadir echo removal in synthetic aperture radar via waveform diversity and dual-focus postprocessing," *IEEE Geosci. Remote Sens. Lett.*, vol. 15, no. 5, pp. 719–723, May 2018.